

Adsorption of Atmospherically Relevant Gases at the Air/Water Interface: Free Energy Profiles of Aqueous Solvation of N₂, O₂, O₃, OH, H₂O, HO₂, and H₂O₂

Robert Vácha,[†] Petr Slavíček,^{†,§} Martin Mucha,[†] Barbara J. Finlayson-Pitts,[‡] and Pavel Jungwirth^{*,†}

Institute of Organic Chemistry and Biochemistry, Academy of Sciences of the Czech Republic and Center for Complex Molecular Systems and Biomolecules, Flemingovo nám. 2, 16610 Prague 6, Czech Republic, and Department of Chemistry, University of California, Irvine, California 92697-2025

Received: August 19, 2004; In Final Form: October 19, 2004

Free energy profiles associated with moving atmospheric gases or radicals across the air/water interface were calculated as potentials of mean force by classical molecular dynamics simulations. With the employed force field, the experimental hydration free energies are satisfactorily reproduced. The main finding is that both hydrophobic gases (nitrogen, oxygen, and ozone) and hydrophilic species (hydroxyl radical, hydroperoxy radical, or hydrogen peroxide) have a free energy minimum at the air/water interface. As a consequence, it is inferred that atmospheric gases, with the exception of water vapor, exhibit enhanced concentrations at surfaces of aqueous aerosols. This has important implications for understanding heterogeneous chemical processes in the troposphere.

1. Introduction

The role of liquid aerosols, such as water microdroplets or aqueous sea salt particles, in the chemistry of the troposphere is being increasingly recognized.¹ The standard picture of aqueous aerosols as tropospheric “mini-reactors” involves the uptake of reactive gases, followed by diffusion and chemical reactions in the aerosol and release of the products back into the atmosphere. It has been shown recently, however, that important tropospheric reactions can take place at the surfaces of liquid aerosols. For example, measurements and modeling studies strongly indicate that the photochemical formation of molecular chlorine in the ozone-containing marine boundary layer is primarily a heterogeneous process occurring at the air/water interface of aqueous sea-salt aerosols.^{2,3}

To quantify chemical processes occurring in liquid aerosols, it is essential to know the atmospheric concentrations of the reactive gases and their solubilities. At low gas concentrations and reactivities, the uptake into the liquid aqueous aerosols can be usually characterized via the corresponding Henry’s law constant, which is directly related to the hydration free energy of the particular gas.⁴ If cases where the concentration or reactivity of a solvated gas is high are left aside, the use of the Henry’s law constant can also be improper for reactions occurring at the surfaces of liquid aerosols. More precisely, it is by no means obvious that the concentration of a reactive gas monotonically switches at the air/water interface from the gas-phase value to that in the aqueous bulk of the aerosols. As a matter of fact, it has been known for almost a century that the surface tension of water slightly decreases with increasing atmospheric pressure, which can be interpreted via the Gibbs

equation in terms of adsorption of nitrogen and/or oxygen at the aqueous surface.⁵ The conditions under which one might expect deviations from Henry’s law due to adsorption of a variety of species, particularly organics, on the surfaces of particles in the atmosphere have been discussed recently by Djikaev and Tabazadeh.⁶

In the present paper, we investigate, by means of molecular dynamics simulations, the process of aqueous solvation of a series of atmospherically relevant gases including nitrogen, oxygen, ozone, hydroxyl radical, water vapor, hydroperoxy radical, and hydrogen peroxide. Solvation of OH and HO₂ in small- and medium-sized water clusters has been studied in recent years by means of ab initio quantum chemistry methods and IR spectroscopy,^{7–10} while the uptake of OH, O₃, and HO₂ at aqueous surfaces was most recently modeled within kinetic molecular dynamics studies.^{11–13} Here, we evaluate the free energy profiles (i.e., the so-called potentials of mean force^{14,15}) associated with transporting the gas molecule across the extended air/water interface into the aqueous bulk, with emphasis on the behavior at the aqueous surface. We show that almost all of these gases exhibit a surface free energy minimum and, consequently, a concentration enhancement at the air/water interface, which has important implications for heterogeneous tropospheric chemistry.

2. Computational Approach

For investigation of the aqueous solvation of atmospheric gases, we used classical molecular dynamics (MD) simulations performed using the program package *Gromacs 3.1.5*.¹⁶ For each of the gas species, we calculated the potential of mean force (PMF), that is, the free energy profile ΔG connected with moving the molecule from the gas phase, through an aqueous slab, and back to the gas phase. From the free energy difference between points 1 and 2 at the path (e.g., in the liquid, at the surface, or in the gas phase), one can evaluate the molecular concentration ratio of the solute at these points

* To whom correspondence should be addressed. E-mail: pavel.jungwirth@uochb.cas.cz.

[†] Academy of Sciences of the Czech Republic and Center for Complex Molecular Systems and Biomolecules.

[‡] University of California.

[§] Present address: Department of Chemistry, University of Illinois, Urbana, IL 61801.

$$\frac{c_1}{c_2} = \exp(-\Delta G_{12}/RT) \quad (1)$$

If we take one point in the liquid and the other in the gas phase, the calculated ratio can be compared to the experimental Henry's law constant. Here, we adopt a definition where the Henry's law constant is given as the concentration of a molecule in the liquid divided by its partial pressure in the gas phase:⁴

$$k_H = \frac{c_1}{p_g} \quad (2)$$

Henry's law can, however, also be written in dimensionless form as a ratio between molecular concentrations in the liquid and gas phases:

$$k_H^{cc} = \frac{c_1}{c_g} \quad (3)$$

There is a simple relation between these two constants and the solvation free energy of the molecular species at infinite dilution:

$$k_H^{cc} = k_H \cdot RT = \exp(-\Delta G_{\text{solv}}/RT) \quad (4)$$

Here, R is the universal gas constant, T stands for temperature, c_1 and c_g are concentrations in the liquid and gas phases, k_H is the Henry's law constant, and ΔG_{solv} is the solvation free energy, which can be directly compared to our calculations. Note that the standard solvation free energies (at $p_0 = 1$ atm gas pressure and $c_0 = 1$ M concentration) differ from those corresponding to a single gas molecule (i.e., pertinent to the present simulations) by a factor of $RT \ln(RTc_0/p_0) = 1.9$ kcal/mol.¹⁷ The values of Henry's law constants used in this study were taken from a compilation by Sander.¹⁸

3. Computational Details and Potential Parameters

Our system consisted of an atmospherically relevant molecule or radical (H_2O , N_2 , O_2 , O_3 , HO , HO_2 , or H_2O_2) and 215 water molecules. Water was placed in a rectangular cell with dimensions of $18.6 \times 18.6 \times 388.6 \text{ \AA}^3$, and periodic boundary conditions were applied, yielding an infinite slab of a 20 \AA thickness in the z -direction, possessing two air/water interfaces. An interaction cutoff of 9 \AA was employed. The effect of long-range Coulomb interactions was accounted for using the smooth particle mesh Ewald summation.¹⁹

We employed the SPC/E model of water.²⁰ For the atmospheric molecules or radicals, we chose among the existing parametrizations (or combinations thereof) which most effectively reproduced the experimental hydration energies. The intermolecular force field parameters together with the relevant references^{11,16,20,21} are summarized in Table 1. When available, the fractional charges and quadrupole moments of the solute molecules were taken from the literature (see Table 1). The remaining fractional charges were estimated using natural population analysis at MP2/aug-cc-pvtz geometries (performed using the *Gaussian 03*²² program). In the cases of OH and ozone, the charges were slightly increased to account for polarization effects and to better reproduce the solvation energies.

The PMF was calculated in the way schematically depicted in Figure 1. A very heavy fictitious particle (X) was connected to the solute molecule (S) and to the center of mass of the water slab (CM). The very heavy fictitious particle defines a stationary point and the pulling direction of the solute. Both harmonic constraints act only in the z -direction normal to the slab surface

TABLE 1: Force Field Parameters

	σ [\AA]	ϵ [kcal/mol]	charge distribution	ref
N_2	4.201	0.1973	-1.740 D\AA (quadrupole)	21
O_2	2.955	0.2029	-0.8081 D\AA (quadrupole)	16
H ₂ O SPC/E				
H	0.000	0.0000	0.4238 e	20
O	3.166	0.1554	-0.8476 e	
O ₃				
O _{center}	2.896	0.2530	0.2400 e	11, 16
O _{side}	2.896	0.2530	-0.1200 e	
OH				
H	0.000	0.0000	0.50 e	16
O	3.166	0.1554	-0.50 e	
HO ₂				
H	0.000	0.0000	0.4454 e	16
O _{center}	2.626	0.4121	-0.4228 e	
O _{side}	2.626	0.4121	-0.0226 e	
H ₂ O ₂				
H	0.000	0.0000	0.4976 e	16
O	3.166	0.1554	-0.4976 e	

(i.e., the resulting force has solely a z -component), thus posing no restriction on the movement of either slab or solute in the xy -plane. The z -component of the X-CM separation is kept constant, thus fixing the water slab in space. By adjusting the z -component of the X-S length, we change the relative distance between the slab and the solute.

The whole simulation consisted of a series of two alternating processes: sampling and pulling. During each of the sufficiently long (1.5 ns) sampling periods, the z -component of the X-S length was harmonically constrained, and the force was monitored and averaged over time. During each of the 20 ps pulling periods, the length was varied by a total of 0.5 \AA . Thus, pulling was carried out sufficiently slowly to ensure that the system does not depart significantly from equilibrium. In about 80 such cycles, the solute molecule was pulled through the whole slab, and the profile of the mean force was obtained. Finally, integrating the force along the z -direction yielded the PMF, with a cumulative error (estimated from the slight asymmetry of the PMF curve with respect to the center of the slab) of ~ 0.3 kcal/mol.

4. Results and Discussion

4.1. General Features of Solvation Free Energy Profiles.

Before presenting separately the free energy profiles of each of the atmospheric molecules or radicals under study, we discuss first their general features. Figure 2 shows a typical PMF together with the corresponding force and water density profile. While the force exhibits a certain statistical noise, its integral (i.e., the PMF) is already a relatively smooth curve. The PMF is defined up to an arbitrary additive constant, which we chose such as to make the free energy equal to zero in the gas phase. It levels off in the bulk liquid at the value of the solvation free energy. Note also the two shallow minima at each of the two air/water interfaces. Ideally, the PMF should be perfectly symmetric with respect to the center of the slab, any asymmetries thus indicating systematic and convergence error margins of the actual calculation.

The PMF is shown again in detail, together with the corresponding concentration profile (see eq 1) in Figure 3. The figure corresponds to a hydrophobic molecule, the free energy of which is lower in the gas phase than in the liquid, and consequently, its population in the aqueous bulk is lower than that in the gas phase. For a hydrophilic molecule or radical, the situation is the opposite. The surface minima at the PMF

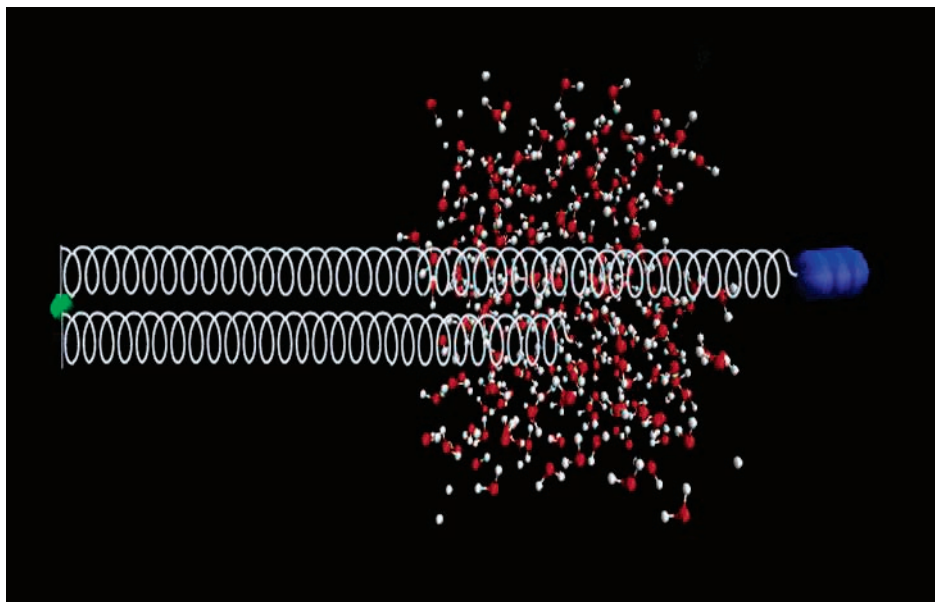


Figure 1. Graphical representation of the computational setup for the calculation of the potential of mean force. Color coding: water molecules (red and white), solute (blue), and the very heavy fictitious particle (green).

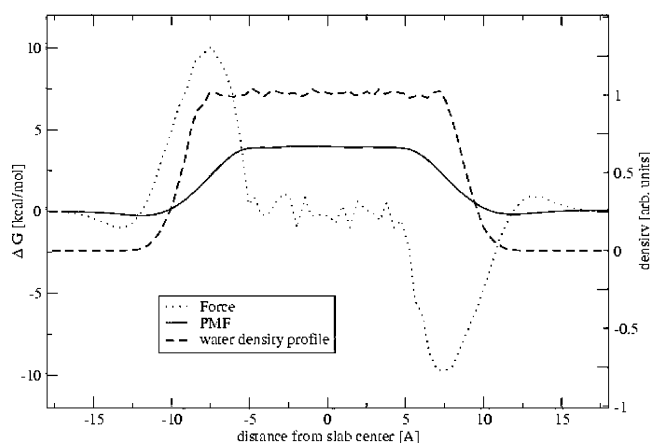


Figure 2. Typical force profile and the corresponding potential of mean force for moving a gas molecule across an aqueous slab of which the extent is characterized by the water density profile.

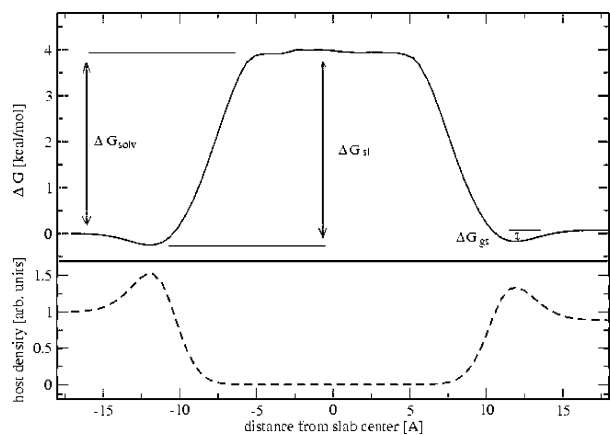


Figure 3. Typical potential of mean force and the corresponding concentration profile for a gas molecule moving across an aqueous slab.

correlate with enhancement of the solute molecule concentration at the two air/water interfaces of the aqueous slab. As demonstrated in the following sections, this surface enhancement is a generic feature of all investigated molecular and radical

species at aqueous interfaces, except for water vapor itself. The three important free energy differences, the solvation (i.e., gas-to-liquid) free energy ΔG_{solv} , the gas-to-surface free energy difference ΔG_{gs} , and the surface-to-liquid free energy difference ΔG_{sl} , are also defined in Figure 3. Only two of these values are independent, as $\Delta G_{\text{solv}} = \Delta G_{\text{gs}} + \Delta G_{\text{sl}}$.

4.2. Hydrophobic Molecules. Out of the seven atmospheric gases under study, three are hydrophobic (i.e., their solvation free energy is positive). These are N_2 , O_2 , and O_3 . Figure 4a depicts the PMF for nitrogen together with the water density profile defining the extent of the aqueous slab. We see that the simulation satisfactorily reproduces the solvation free energy of +2.5 kcal/mol derived from the experimental Henry's law constant. Curves exhibit surface minima implying an enhanced concentration of N_2 at the air/water interface compared to the gas phase. This surfactant behavior of nitrogen is consistent with the slight decrease of surface tension of water upon increasing the atmospheric pressure (by about $0.1 \text{ mN m}^{-1} \text{ atm}^{-1}$).⁵

The PMF of molecular oxygen (see Figure 4b) is similar to that of nitrogen. The employed force field reproduces well the experimental solvation free energy of +2.0 kcal/mol. As in the previous case, a surface minimum develops with a depth of more than 0.5 kcal/mol, which corresponds at 300 K to a 240% enhancement of O_2 at the air/water interface compared to the gas phase. In agreement with previous studies,²³ a very weak barrier (of less than 0.25 kcal/mol) between the aqueous bulk and the surface region seems to develop at the PMF. Note, however, that the height of this barrier is probably within the error of the calculation.

Ozone is much less hydrophobic than the two dominant atmospheric gases with an experimental solvation energy of +0.7–0.9 kcal/mol, which is reproduced also by the present calculations (see Figure 4c). At the same time, the surface minimum is deeper than in the case of O_2 or N_2 , reaching 1.2 kcal/mol. This corresponds, at an ambient temperature, to a roughly sevenfold increase of ozone concentration at the air/water interface compared to the gas phase. This surfactant activity is in accord with the results of our previous dynamical study of ozone uptake at aqueous surfaces.¹¹ As in the case of molecular oxygen, a very weak (if any) barrier between the bulk region and the surface occurs on the PMF of ozone.

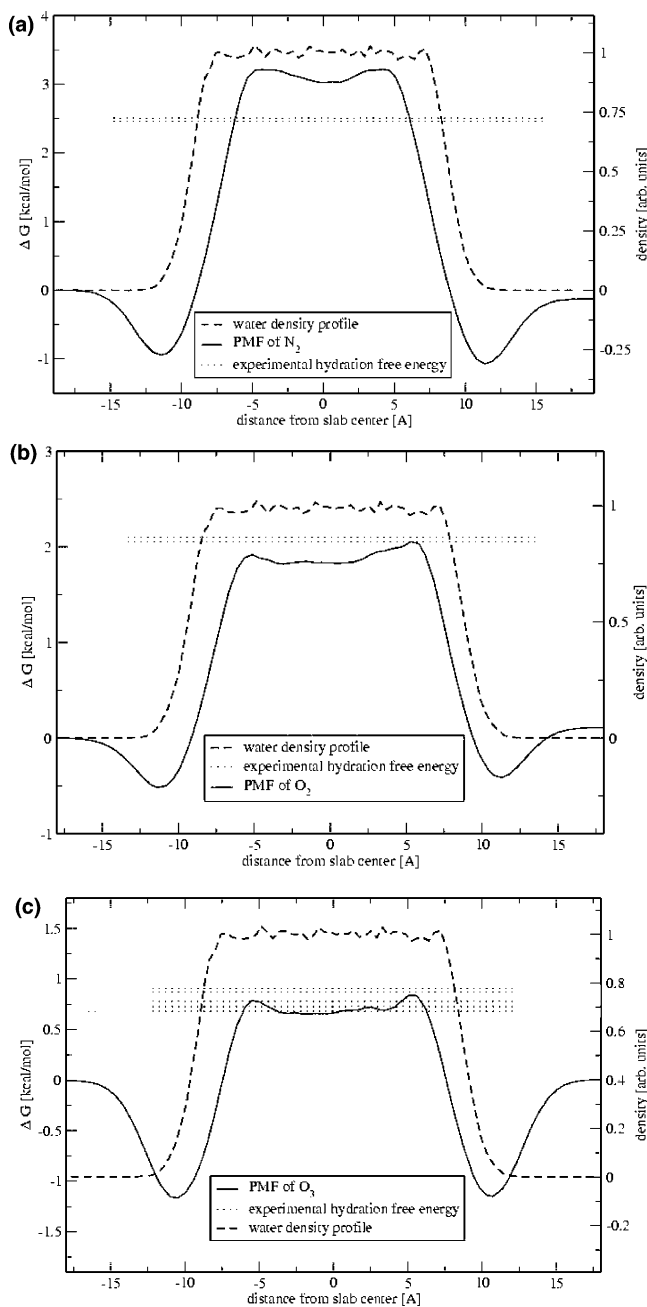


Figure 4. Potential of mean force for moving (a) N_2 , (b) O_2 , and (c) O_3 through an aqueous slab defined via the water density profile. The experimental hydration energies obtained from the Henry's law constants in several measurements are displayed as horizontal lines.¹⁸

4.3. Hydrophilic Molecules and Radicals. The hydrophilic gases under investigation (the solvation free energy of which is negative) comprise hydroxyl radical, water vapor, hydroperoxy radical, and hydrogen peroxide. All of these four gaseous species have a lower free energy in water than in the air, the hydration energy of the last two being even larger than that of a water molecule. Figure 5a depicts the PMF for the OH radical. The experimental hydration energy of roughly -4 kcal/mol is reasonably well reproduced by the calculation. Also, note the relatively very deep surface minimum of about 1.4 kcal/mol, corresponding to an order of magnitude concentration enhancement of OH at the surface compared to the aqueous bulk. Results from the present PMF calculations thus support previous dynamical studies of the uptake of hydroxyl radical at aqueous surfaces.^{9,10}

For water vapor, the hydration free energy from the present calculations agrees well with the chemical potential of H_2O of -6.3 kcal/mol (see Figure 5b).¹⁷ No appreciable (above statistical and systematic error) surface minimum is observed on the PMF (water is, of course, not a surfactant on water).^{12,14}

A somewhat surprising fact is that even gases more hydrophilic than water vapor itself, such as hydroperoxy radical and hydrogen peroxide, develop a free energy minimum at the aqueous surface (see Figure 5c,d). This is particularly remarkable for the HO_2 radical, which exhibits a surface minimum of about one-half the magnitude of that of the less hydrophilic OH radical, while the surface free energy minimum of H_2O_2 is somewhat smaller. Finally, note that in the cases of both hydroperoxy radical and hydrogen peroxide the hydration free energies derived from the experimental Henry's law constants are well-reproduced by the present calculations.

4.4. Summary of Calculations. The results of calculations are summarized in Table 2, which shows for each of the gases under investigation their aqueous bulk concentration and its highest value in the interfacial region, both normalized to the gas-phase value. These values were obtained by converting the potentials of mean force into concentration profiles using eq 1, assuming temperature of 300 K. The table also shows the concentrations averaged over the surface peak area together with the corresponding peak width. These mean surface concentrations are understandably lower than the peak values; nevertheless, the sizable surface enhancement, observed for most of the gases under study, pertains. As far as the orientation of the solute molecules at the interface is concerned, hydrophilic molecules tend to be oriented (e.g., OH has the hydrogen atom pointing toward the bulk phase), while the investigated hydrophilic molecules do not show any strong orientational preference.

4.5. Implications for Atmospheric Chemistry. The enhancement of inorganic species at the air/water interface has some potentially important implications for reactions at the surfaces of particles in the atmosphere. In the troposphere, oxidation is well-known to occur in the gas phase and in the bulk liquid phase of particles, fogs, and cloud droplets.¹ The major oxidants are the hydroxyl radical and, in coastal marine areas, atomic chlorine (primarily during the day), the nitrate radical (primarily at night), and ozone (both day and night). In addition, H_2O_2 and to a lesser extent organic hydroperoxides are important in the aqueous phase for the oxidation of dissolved SO_2 , for example.

However, over the past decade, it has also been recognized that unique species and reactions of inorganics can occur at the air/water interface.^{2,24–32} In addition, it has been proposed that organic compounds can be scavenged onto the surfaces of cloud droplets, resulting in higher net uptake of organics than expected on the basis of a Henry's law equilibrium.⁶ The calculations presented here show that oxidants such as OH and O_3 are also expected to be enhanced in this region. The combination of oxidizable surface species along with enhanced concentrations of atmospheric oxidants at the interfaces of particles, fog, and cloud droplets may play a significant role in the atmospheric processing of some organics as well as inorganic species.

For example, in recent field studies of clouds interacting with a plume from biomass burning, the rapid oxidation of methanol to formaldehyde was observed.³³ This was much larger than predicted from gas and bulk aqueous-phase chemistry, and Tabazadeh and co-workers suggested that it was due to heterogeneous processes. At a gas-phase OH concentration³⁴ of 2×10^7 OH cm^{-3} , the equilibrium concentration of OH in the bulk phase of the cloud droplets would be 3.1×10^{-11} mol

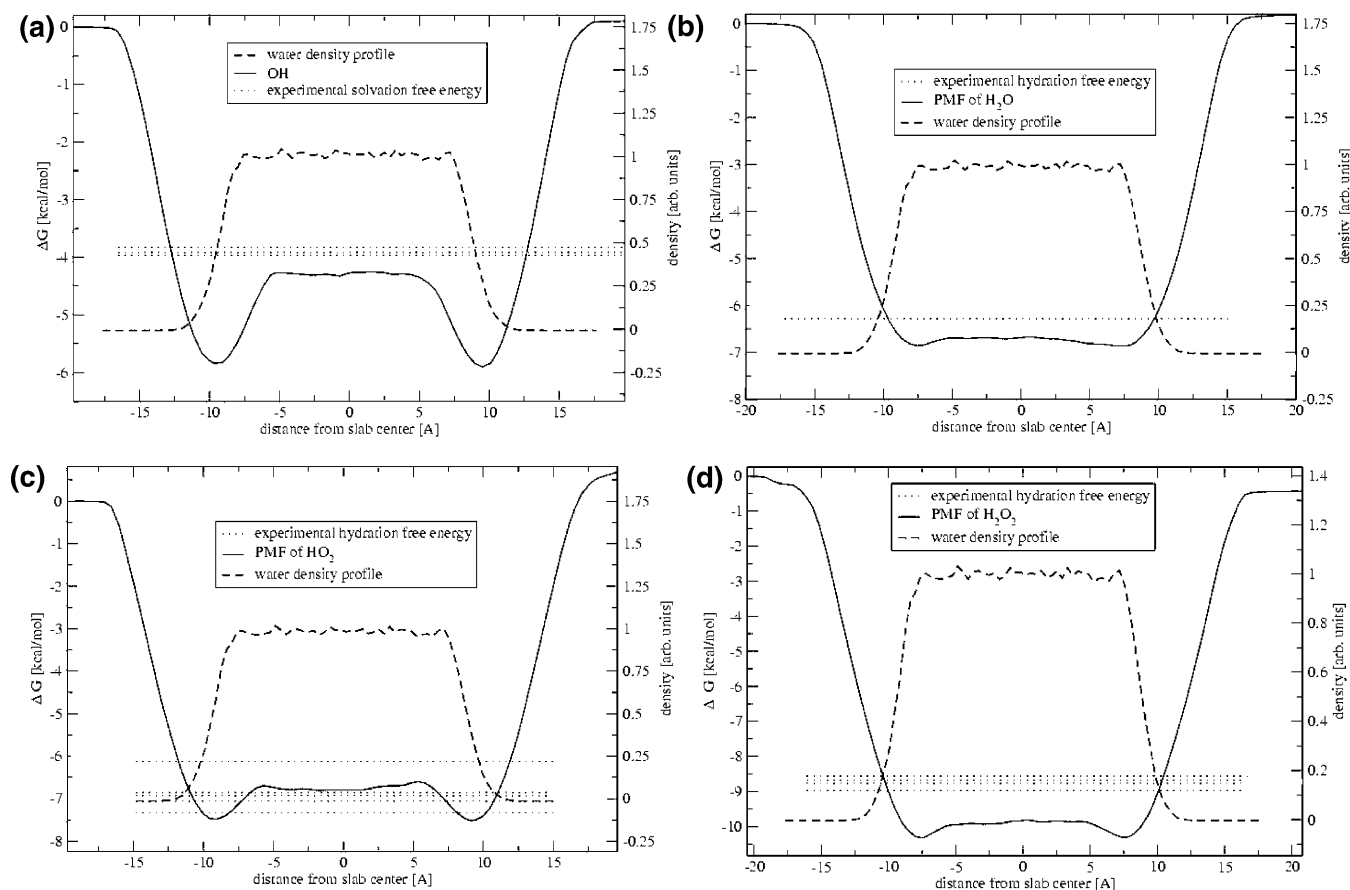


Figure 5. Potential of mean force for moving (a) OH, (b) H₂O, (c) HO₂, and (d) H₂O₂ through an aqueous slab defined via the water density profile. The experimental hydration energies obtained from the Henry's law constants in several measurements are displayed as horizontal lines.¹⁸

TABLE 2: Aqueous Bulk Concentrations and Their Highest and Averaged Values in the Interfacial Region^a Compared to the Gas-Phase Value for Seven Important Atmospheric Gases.

gas phase	aqueous bulk	aqueous surface: highest value	aqueous surface: averaged value	width of the interfacial peak (Å)	
N ₂	1.0	0.010	4.9	3.21	5.7
O ₂	1.0	0.046	2.4	1.76	5.7
O ₃	1.0	0.33	7.1	3.62	8.3
OH	1.0	1 100	11 000	8 800	6.9
H ₂ O	1.0	75 000	75 000	75 000	0
HO ₂	1.0	90 000	290 000	206 000	4.4
H ₂ O ₂	1.0	17 000 000	34 000 000	25 700 000	3.7

^aThe width of which is defined as the width of the interfacial peak of the population of the solute species.

L⁻¹ (using a Henry's law constant of 39 M atm⁻¹). On the basis of the present calculations of the mean enhancement of OH at the interface by a factor of 8 (see Table 2), the OH concentration in the interfacial region would be 2.5×10^{-10} mol L⁻¹. We take the interfacial width to be our calculated value of 6.9 Å and the cloud surface area to be 6.3×10^{-3} cm² cm⁻³ as reported by Tabazadeh et al.³³ If the rate constant for oxidation of CH₃OH by OH in the bulk aqueous phase ($k = 8 \times 10^8$ M⁻¹ s⁻¹ at -5 °C measured in the clouds)³⁵ is applicable to the interfacial region, then the observed rate of loss of gas-phase CH₃OH from 36 to 15 ppb in 3 min could be accomplished at the interface if the methanol surface coverage was ~0.4% of a monolayer and if there was no diffusion limitation for replenishing the methanol at the interface. While this surface coverage of methanol might not be expected for pure water droplets,³⁶ these clouds were heavily impacted by a biomass burning plume^{33,34} which contains substantial amounts of organics in both the gas phase and particles.¹ These would be expected to lead to an increased uptake of methanol, and given the dense

smoke plumes during these measurements, significant availability of the alcohol for oxidation at the interface is feasible.

A second example is the oxidation of polycyclic aromatic hydrocarbons (PAHs) on the surfaces of particles, fogs, and clouds. The vapor pressures of PAHs are such that the smaller PAHs exist totally in the gas phase, while the larger ones are in the particle phase; PAHs of intermediate size and vapor pressures are semivolatile and partition between the two phases.¹ For those that partition in whole or in part to particles, oxidation at the interface can be an important loss process in the atmosphere.

For example, Donaldson and co-workers^{37,38} have shown that anthracene on water or aqueous solutions containing alcohols or acids is oxidized on exposure to gas-phase O₃. The kinetics suggests that the mechanism involves the initial adsorption/desorption of ozone followed by oxidation of anthracene by the surface-adsorbed O₃ in a Langmuir-Hinshelwood type of process. Donaldson and co-workers³⁸ report that at 50 ppb O₃, the effective reaction probability is in the range $(0.2-3) \times 10^{-7}$

depending on the composition of the underlying solution. For an air parcel containing 10^4 particles of 1- μm diameter per cm^3 of air, the loss of anthracene at the surface would be 3.5×10^3 molecules per cubic centimeter of air per second if the surface coverage of the anthracene is 1%. This can be compared to the gas-phase rate of oxidation calculated to be 9×10^2 anthracene per cubic centimeter of air per second by OH (taken as $5 \times 10^6 \text{ cm}^{-3}$)¹ for an initial gas-phase anthracene concentration of $1 \times 10^7 \text{ cm}^{-3}$. One reason for the unusually rapid oxidation of anthracene observed by Donaldson and co-workers³⁸ at the interface may be the enhancement of ozone in the interfacial region, which the present calculations suggest is about 1 order of magnitude compared to its bulk concentration. While the coverage of anthracene on particles in air is not known, it is likely that there will be cases such as biomass plumes (discussed already for methanol) and organics present on the surfaces of urban and sea salt particles^{39,40} that may lead to enhanced uptake of other organics such as the PAHs.

A further potential consequence of the enhancement of O_3 in the interface region is the increased production of OH and OH precursors such as H_2O_2 by photolysis of O_3 .¹ When combined with the enhancement at the interface of other OH photochemical sources such as the nitrate ion,⁴¹ the potential for increased oxidative capacity at the surface of particles, fogs, and clouds is even more evident.

Clearly, the relative importance of gas, bulk liquid phase, and interface oxidations will depend on a number of factors such as gas-phase concentrations, Henry's law constants, and the surface coverage of the organic. For example, while naphthalene has been reported to be enhanced at the air/water interface,⁴² its high vapor pressure¹ is such that oxidation at the interface or in the bulk of particles cannot compete with the gas-phase oxidation by OH. However, for less volatile compounds, the gas-phase processes become less important, and the interface chemistry becomes relatively more so.

Finally, not all oxidants are significantly enhanced at the surface. For example, the present studies suggest that H_2O_2 is only increased in the interfacial region by $\sim 50\%$ compared to the bulk. Hydrogen peroxide is known to be a major aqueous-phase oxidant for SO_2 [known as S(IV)] dissolved in fogs and clouds in the atmosphere.¹ The lack of a substantial increase in the predicted concentration of H_2O_2 at the interface is consistent with the experimental observation⁴³ that a surface reaction of H_2O_2 with SO_2 does not appear to be important compared to oxidation in the bulk, despite the existence of an S(IV) surface complex.^{24,26,29,30}

In short, while our understanding of the importance of oxidations at the air/water interface of particles, fogs, and clouds is in its infancy, the present calculations of enhanced oxidant concentrations in the interfacial region suggest that it is an area that should be pursued further.

5. Conclusions

We have calculated by means of molecular dynamics simulations the potentials of mean force connected with moving an atmospherically relevant molecule or radical (N_2 , O_2 , O_3 , OH, H_2O , HO_2 , or H_2O_2) through an aqueous slab. The hydration free energies, as inferred from the experimental Henry's law constants, are well-reproduced by the simulations. The present calculations indicate that the propensity of gaseous molecules and radicals for the air/water interface is a generic effect, present for both hydrophobic and hydrophilic species. The only exception is water vapor itself, which does not show, beyond statistical uncertainty, any surface free energy minimum, in agreement with common sense and previous calculations.^{14,44}

At the interface, solute molecules can exploit attractive (van der Waals and electrostatic) interactions with the solvent, without significantly disturbing the hydrogen-bonded structure of water. Out of the three phases involved (gas, liquid, and interface) the gaseous molecules other than water thus have the highest concentration at the aqueous surface with a population enhancement with respect to the second most populated phase ranging from a factor of ~ 2 (e.g., for O_2) to a factor of ~ 10 (e.g., for OH). The calculated depth of the surface free energy minimum depends to some extent on the particular choice of force field, however, this "physisorption" at the air/water interface is likely to be generally present for almost all gaseous species. The surface enhancement of atmospherically relevant gases has possible important consequences for heterogeneous atmospheric chemical processes occurring on aqueous aerosols and should be thus considered when interpreting the results of field measurements as well as in tropospheric models.

Acknowledgment. Support from the Czech Ministry of Education via grant no. ME644 and from the US-NSF (grants CHE 0209719 and 0431512) is gratefully acknowledged. Part of the work in Prague has been completed within the framework of research project Z4 055 905. We thank Doug Tobias, Martina Roeselova, John Vieceli, Robert Yokelson, and Azadeh Tabazadeh for valuable discussions. We are also grateful to D. J. Donaldson for helpful discussions and for sharing preprints prior to publication.

References and Notes

- (1) Finlayson-Pitts, B. J.; Pitts, J. N. *Chemistry of the Upper and Lower Atmosphere – Theory, Experiments, and Applications*; Academic Press: San Diego, 2000.
- (2) Knipping, E. M.; Lakin, M. J.; Foster, K. L.; Jungwirth, P.; Tobias, D. J.; Gerber, R. B.; Dabdub, D.; Finlayson-Pitts, B. J. *Science* **2000**, *288*, 301–306.
- (3) Finlayson-Pitts, B. J. *Chem. Rev.* **2003**, *103*, 4801.
- (4) Sander, R. *Surv. Geophys.* **1999**, *20*, 1.
- (5) Defay, R.; Prigogine, I. *Surface tension and adsorption*; Wiley: New York, 1966.
- (6) Djikaev, Y. S.; Tabazadeh, A. *J. Geophys. Res., [Atmos.]* **2003**, *108*, 4689.
- (7) Hamad, S.; Lago, S.; Mejias, J. A. *J. Phys. Chem. A* **2002**, *106*, 9104.
- (8) Cooper, P. D.; Kjaergaard, H. G.; Langford, V. S.; McKinley, A. J.; Quickenden, T. I.; Schofield, D. P. *J. Am. Chem. Soc.* **2003**, *125*, 6048.
- (9) Belair, S. D.; Hernandez, H.; Francisco, J. S. *J. Am. Chem. Soc.* **2004**, *126*, 3024.
- (10) Shi, Q. C.; Belair, S. D.; Francisco, J. S.; Kais, S. *Proc. Natl. Acad. Sci. U.S.A.* **2003**, *100*, 9686.
- (11) Roeselova, M.; Jungwirth, P.; Tobias, D. J.; Gerber, R. B. *J. Phys. Chem. B* **2003**, *107*, 12690.
- (12) Roeselova, M.; Vieceli, J. S.; Dang, L. X.; Tobias, D. J. *J. Am. Chem. Soc.* submitted for publication, 2004.
- (13) Morita, A.; Kanaya, Y.; Francisco, J. S. *J. Geophys. Res., [Atmos.]* **2004**, *109*, 09201.
- (14) Dang, L. X.; Garrett, B. C. *Chem. Phys. Lett.* **2004**, *385*, 309.
- (15) Bader, J. S.; Chandler, D. *J. Phys. Chem.* **1992**, *96*, 6423.
- (16) Lindahl, E.; Hess, B.; van der Spoel, D. *J. Mol. Model.* **2001**, *7*, 306.
- (17) Ben Naim, A.; Marcus, Y. *J. Chem. Phys.* **1984**, *81*, 2016.
- (18) Sander, R. *Compilation of Henry's Law Constants for Inorganic and Organic Species of Potential Importance in Environmental Chemistry*, version 3; www.mpch-mainz.mpg.de/~sander/res/henry.html (accessed 1999).
- (19) Essmann, U.; Perera, L.; Berkowitz, M. L.; Darden, T.; Lee, H.; Pedersen, L. G. *J. Chem. Phys.* **1995**, *103*, 8577.
- (20) Berendsen, H. J. C.; Grigera, J. R.; Straatsma, T. P. *J. Phys. Chem.* **1987**, *91*, 6269.
- (21) Jordan, P. C.; Van Maaren, P. J.; Mavri, J.; Van der Spoel, D.; Berendsen, H. J. C. *J. Chem. Phys.* **1995**, *103*, 2272.
- (22) Frisch, M. J.; Trucks, G. W.; Schlegel, H. B.; Scuseria, G. E.; Robb, M. A.; Cheeseman, J. R.; Montgomery, J. A., Jr.; Vreven, T.; Kudin, K. N.; Burant, J. C.; Millam, J. M.; Iyengar, S. S.; Tomasi, J.; Barone, V.; Mennucci, B.; Cossi, M.; Scalmani, G.; Rega, N.; Petersson, G. A.;

- Nakatsuji, H.; Hada, M.; Ehara, M.; Toyota, K.; Fukuda, R.; Hasegawa, J.; Ishida, M.; Nakajima, T.; Honda, Y.; Kitao, O.; Nakai, H.; Klene, M.; Li, X.; Knox, J. E.; Hratchian, H. P.; Cross, J. B.; Adamo, C.; Jaramillo, J.; Gomperts, R.; Stratmann, R. E.; Yazyev, O.; Austin, A. J.; Cammi, R.; Pomelli, C.; Ochterski, J. W.; Ayala, P. Y.; Morokuma, K.; Voth, G. A.; Salvador, P.; Dannenberg, J. J.; Zakrzewski, V. G.; Dapprich, S.; Daniels, A. D.; Strain, M. C.; Farkas, O.; Malick, D. K.; Rabuck, A. D.; Raghavachari, K.; Foresman, J. B.; Ortiz, J. V.; Cui, Q.; Baboul, A. G.; Clifford, S.; Cioslowski, J.; Stefanov, B. B.; Liu, G.; Liashenko, A.; Piskorz, P.; Komaromi, I.; Martin, R. L.; Fox, D. J.; Keith, T.; Al-Laham, M. A.; Peng, C. Y.; Nanayakkara, A.; Challacombe, M.; Gill, P. M. W.; Johnson, B.; Chen, W.; Wong, M. W.; Gonzalez, C.; Pople, J. A. *Gaussian 03*, revision B.01; Gaussian, Inc.: Pittsburgh, PA, 2003.
- (23) Taylor, R. S.; Ray, D.; Garrett, B. C. *J. Phys. Chem. B* **1997**, *101*, 5473.
- (24) Jayne, J. T.; Davidovits, P.; Worsnop, D. R.; Zahniser, M. S.; Kolb, C. E. *J. Phys. Chem.* **1990**, *94*, 6041.
- (25) Hu, J. H.; Shi, Q.; Davidovits, P.; Worsnop, D. R.; Zahniser, M. S.; Kolb, C. E. *J. Phys. Chem.* **1995**, *99*, 8768.
- (26) Donaldson, D. J.; Guest, J. A.; Goh, M. C. *J. Phys. Chem.* **1995**, *99*, 9313.
- (27) Hanson, D. R.; Ravishankara, A. R. *J. Phys. Chem.* **1994**, *98*, 5728.
- (28) George, C.; Behnke, W.; Scheer, V.; Zetzsch, C.; Magi, L.; Ponche, J. L.; Mirabel, P. *Geophys. Res. Lett.* **1995**, *22*, 1505.
- (29) Boniface, J.; Shi, Q.; Li, Y. Q.; Cheung, J. L.; Rattigan, O. V.; Davidovits, P.; Worsnop, D. R.; Jayne, J. T.; Kolb, C. E. *J. Phys. Chem. A* **2000**, *104*, 7502.
- (30) Clegg, S. M.; Abbatt, J. P. D. *J. Phys. Chem. A* **2001**, *105*, 6630.
- (31) Katrib, Y.; Deiber, G.; Schweitzer, F.; Mirabel, P.; George, C. *J. Aerosol Sci.* **2001**, *32*, 893.
- (32) Strekowski, R. S.; Remorov, R.; George, C. *J. Phys. Chem. A* **2003**, *107*, 2497.
- (33) Tabazadeh, A.; Yokelson, R. J.; Singh, H. B.; Hobbs, P. V.; Crawford, J. H.; Iraci, L. T. *Geophys. Res. Lett.* **2004**, *31*, 06114.
- (34) Hobbs, P. V.; Sinha, P.; Yokelson, R. J.; Christian, T. J.; Blake, D. R.; Gao, S.; Kirchstetter, T. W.; Novakov, T.; Pilewskie, P. *J. Geophys. Res., [Atmos.]* **2003**, *108*, 8485.
- (35) Elliot, A. J.; McCracken, D. J. *Radiat. Phys. Chem.* **1989**, *33*, 69. *NIST Standard Reference Database 40*, 2004.
- (36) Donaldson, D. J.; Anderson, D. *J. Phys. Chem. A* **1999**, *103*, 871.
- (37) Mmereki, B. T.; Donaldson, D. J. *J. Phys. Chem. A* **2003**, *107*, 11038.
- (38) Mmereki, B. T.; Donaldson, D. J.; Gilman, J. B.; Eliason, T. L.; Vaida, V. *Atmos. Environ.*, submitted for publication.
- (39) Tervahattu, H.; Hartonen, K.; Kerminen, V. M.; Kupiainen, K.; Aarnio, P.; Koskentalo, T.; Tuck, A. F.; Vaida, V. *J. Geophys. Res., [Atmos.]* **2002**, *107*, 4053.
- (40) Tervahattu, H.; Juhanoja, J.; Kupiainen, K. *J. Geophys. Res., [Atmos.]* **2002**, *107*, 4319.
- (41) Salvador, P.; Curtis, J. E.; Tobias, D. J.; Jungwirth, P. *Phys. Chem. Chem. Phys.* **2003**, *5*, 3752.
- (42) Raja, S.; Valsaraj, K. T. *Environ. Sci. Technol.* **2004**, *38*, 763.
- (43) Jayne, J. T.; Gardner, J. A.; Davidovits, P.; Worsnop, D. R.; Zahniser, M. S.; Kolb, C. E. *J. Geophys. Res., [Atmos.]* **1990**, *95*, 20559.
- (44) Taylor, S. R.; Garrett, B. C. *J. Phys. Chem. B* **1999**, *103*, 844.